Neuron, Volume *101*

Supplemental Information

Calcium Influx through Plasma-Membrane Nanoruptures Drives Axon Degeneration in a Model of Multiple Sclerosis

Maarten E. Witte, Adrian-Minh Schumacher, Christoph F. Mahler, Jan P. Bewersdorf, Jonas Lehmitz, Alexander Scheiter, Paula Sánchez, Philip R. Williams, Oliver Griesbeck, Ronald Naumann, Thomas Misgeld, and Martin Kerschensteiner

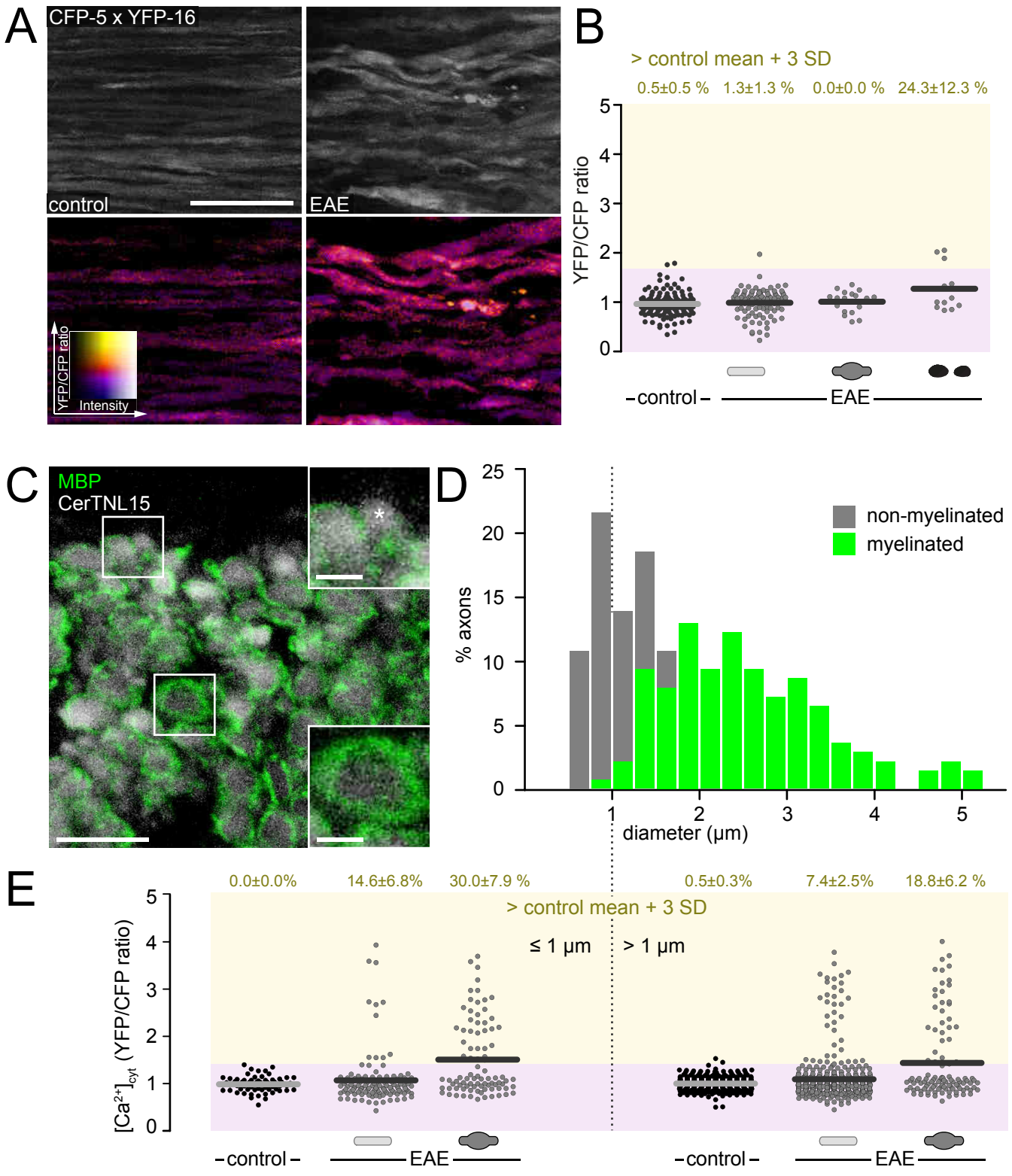

Figure S1 - *In vivo* pH control and axonal characterization related to cytoplasmic calcium measurements in neuroinflammatory lesions (*related to Figure 1*)

(**A**) *In vivo* multiphoton projection images of healthy and EAE *Thy1-CFP-5 x Thy1-YFP16* mice, illustrating that CFP and YFP fluorescence are not differentially affected by the EAE environment (e.g. by pH alterations) **Top:** grayscale image of YFP channel, **bottom:** overlayed ratiometric (YFP/CFP) images. (**B**) YFP/CFP ratios of single axons in healthy (n=2 mice) and acute EAE mice (n=3 mice) normalized to control mean. **Top:** Percentage of axons with YFP/CFP ≥ 3

SD above control mean, shown as mean ± SEM. (**C**) *In situ* confocal projection of a spinal cord cross section of a healthy *Thy1-CerTN-L15* mouse, immuno-labeled with anti-MBP antibody to visualize myelin. **Right:** Boxed detail of non-myelinated (**top,** asterisk) and myelinated axon cross section (**bottom**). (**D**) Quantification of axon diameters of myelinated and non-myelinated axons *in situ* (n=204 axons in 2 mice). (**E**) *In vivo* $[Ca^{2+}]_{cyt}$ of small caliber axons (≤ 1 µm, **left**) vs. large caliber axons (> 1 µm, **right**) in healthy and acute EAE mice, plotted as YFP/CFP channel ratios (normalized to healthy control mean). Percentages indicate $[Ca^{2+}]_{cyt}$ ≥ control mean +3 SD, shown as mean ± SEM (n=6 control mice, n=11 EAE mice; same data set is shown as pooled analysis in **Fig. 1C**). Scale bars in **A**, 25 µm (applies to all images); **C**, 10 µm (overview), 2.5 µm (boxed images).

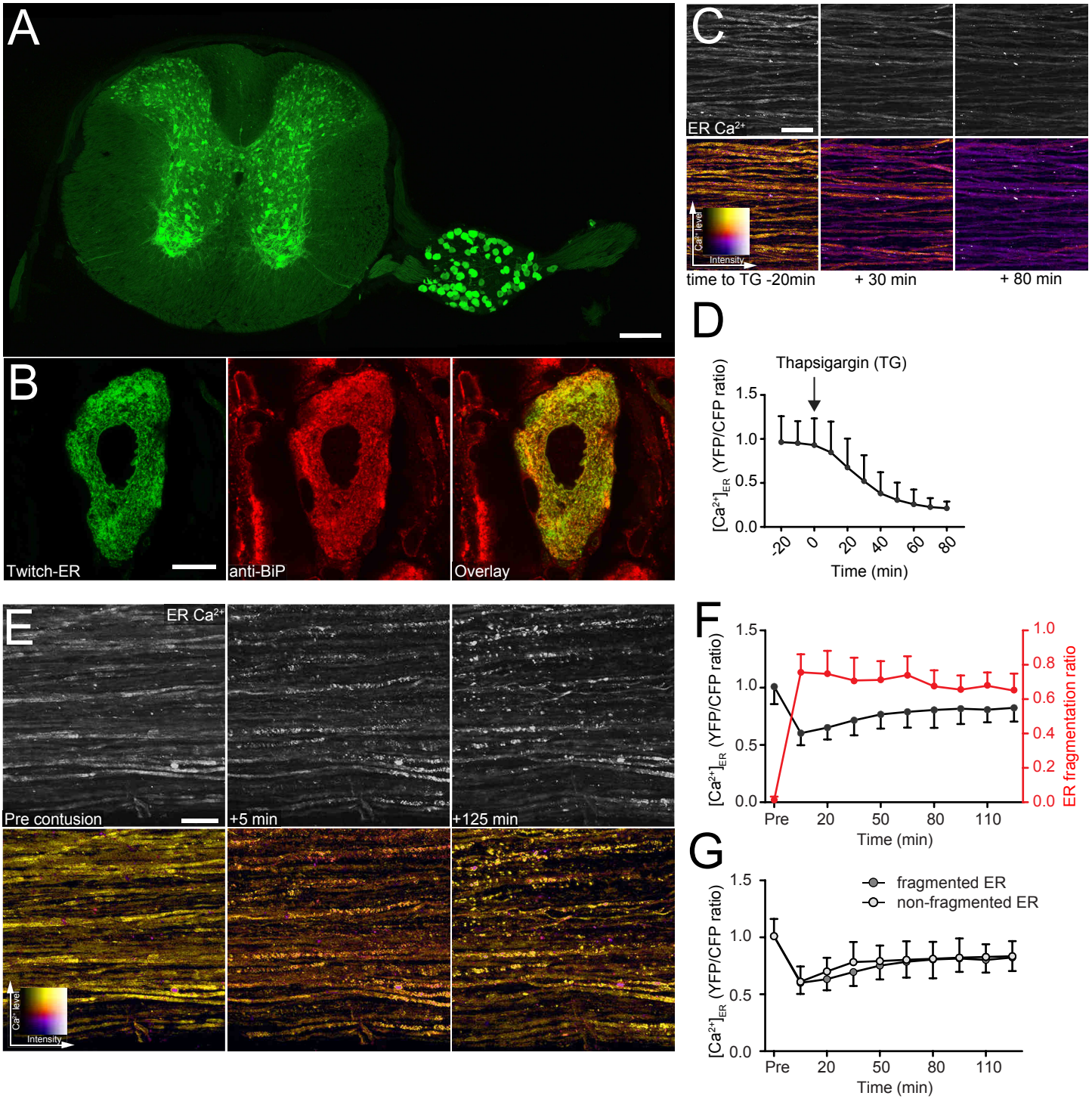

Figure S2 – Histological and functional characterization of *Thy1-TwitchER* mice (*related to Figure 2*)

(**A**) Confocal low-magnification projection image of a thoracic spinal cord cross-section with attached dorsal root ganglion (DRG) of a *Thy1-TwitchER* mouse. (**B**) Single DRG neuronal soma showing pattern of Twitch-ER fluorescence (green, **left**) and staining pattern of anti-BiP immuno-labeling for ER (red, **middle**) and an overlay of both channels (**right**). (**C**) Time-lapse *in vivo* images of axons in the spinal cord of a *Thy1-TwitchER* mouse before and after application of 100 µM thapsigargin (TG). Projection images, for YFP channel in greyscale (**top**), ratiometric (YFP/CFP) images color coded for ER calcium levels ($[Ca^{2+}]_{ER}$, **bottom**). (**D**) Time course of $[Ca^{2+}]_{ER}$ pre and post thapsigargin application, measured every

10 min (n=4 mice) and presented as mean + SD. (**E**) *In vivo* multiphoton projection images of spinal cord axons of healthy *Thy1-TwitchER* mice before ('Pre contusion'), 5 min ('+5 min') and 125 min ('+125 min') after spinal cord contusion (**top:** greyscale images of YFP channel, **bottom:** overlayed ratiometric (YFP/CFP) images color-coded for $[Ca^{2+}]_{ER}$). (**F**, **G**) Time course (pre and post contusion of the spinal cord) of $[Ca^{2+}]_{ER}$ measured in spinal axons every 15 mins (n=5 mice) (**F**) YFP/CFP ratios for all axons (**black**, mean - SD) and axonal ER fragmentation ratio (fragmented ER/total ER, **red**, mean + SD). (**G**) YFP/CFP ratios for axons with fragmented ER (**dark grey**, mean - SD) and non-fragmented ER (**light grey**, mean + SD). Scale bars in **A**, 200 µm; **B**, 10 µm; **C, E**, 25 µm.

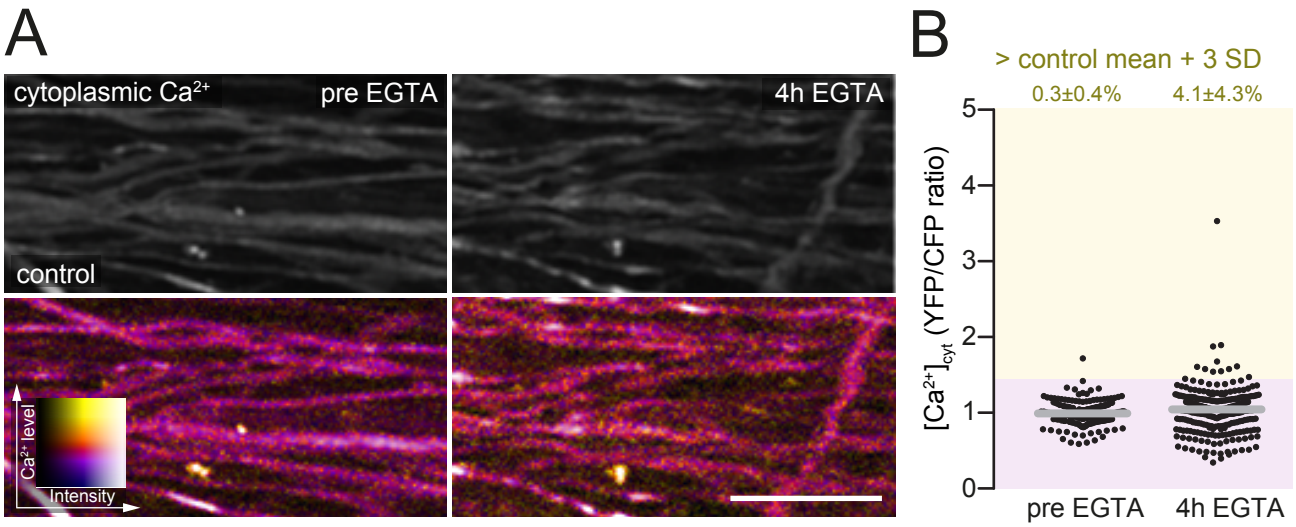

Figure S3 - Application of EGTA does not cause cytoplasmic Ca^{2+} alterations in healthy axons (*related to Figure 3*)

(**A**) *In vivo* multiphoton time-lapse (single time points projection images) of the spinal cord in a healthy *Thy1-CerTN-L15* mouse showing axonal morphology (**top:** greyscale images of YFP channel) and $[Ca^{2+}]_{cyt}$ (**bottom:** overlayed ratiometric YFP/CFP images color-coded for cytoplasmic calcium) before (**left,** 'pre EGTA', incubated in aCSF) and after (**right,** '4h EGTA', 0 Ca^{2+} aCSF containing 50 mM of EGTA) removal of extracellular Ca^{2+}. (**B**) $[Ca^{2+}]_{cyt}$ plotted as YFP/CFP ratio of the same axons before ('pre EGTA', **left**, n=3 mice, 292 axons) and after ('4h EGTA', **right**) removal of extracellular calcium. **Top:** Percentage of axons with $[Ca^{2+}]_{cyt} \geq 3$ SD above control mean, shown as mean ± SEM. No significant differences were observed between the two time points (analyzed by paired t-test). Scale bar in **A**, 10 µm

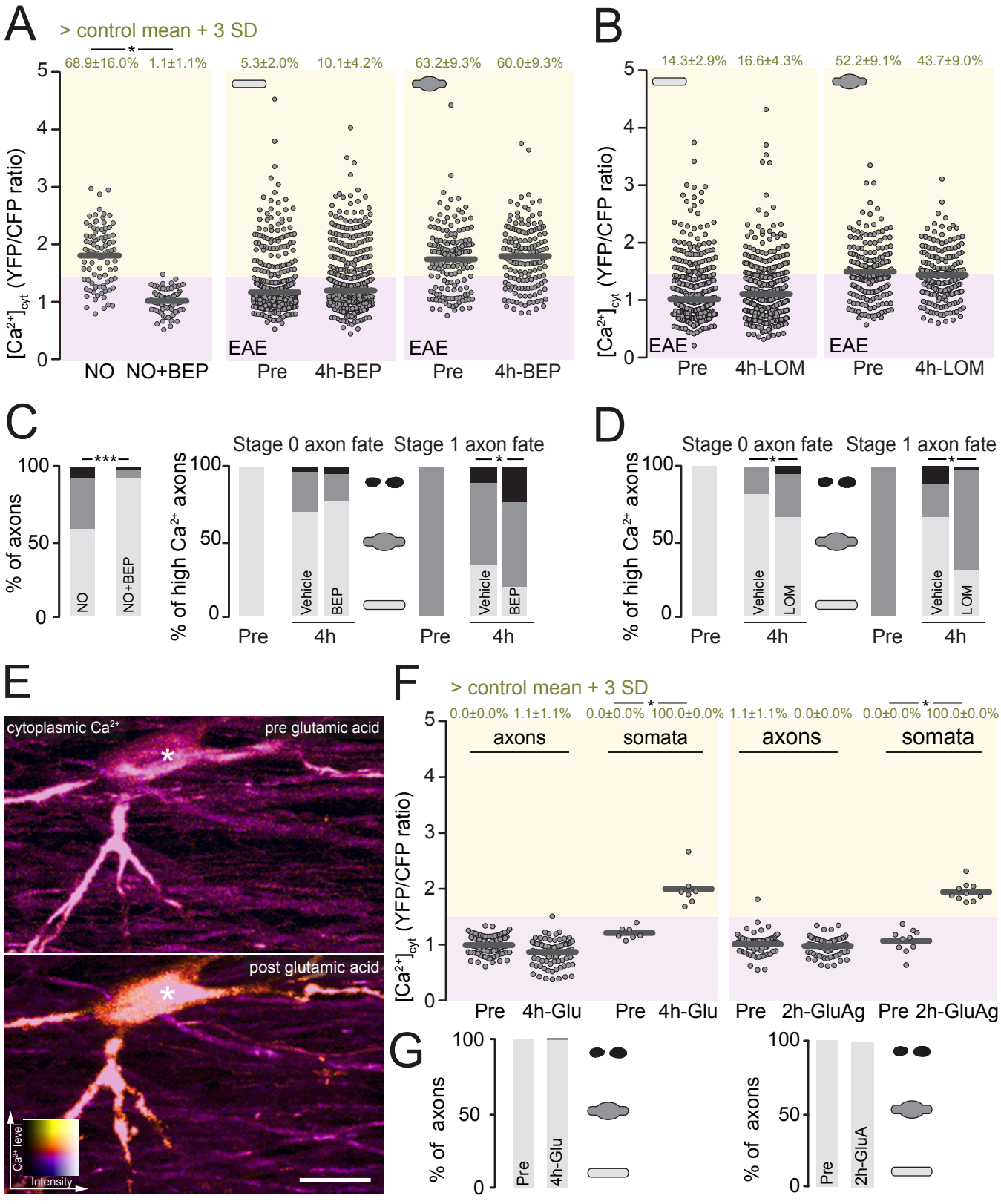

Figure S4 - Inhibition of the Na^+/Ca^{2+}-exchanger (NCX) or voltage-gated Ca^{2+}-channels and application of glutamic acid or glutamate receptor agonists do not alter axonal $[Ca^{2+}]_{cyt}$ (*related to Figure 4*)

(**A**) $[Ca^{2+}]_{cyt}$ of single axons plotted as YFP/CFP ratios. **Left:** after bath-application of a nitric oxide donor ('NO', spermine NONOate 50 mM, 60 min, n=3 mice, 90 axons) and after co-application of a nitric oxide donor and the NCX-inhibitor bep-

ridil ('NO+BEP', spermine NONOate 50 mM, bepridil 0.1 mM, 60 min, n=3 mice, 90 axons) on healthy spinal cord. Stage 0 (**middle**, n=9 mice, 958 axons) and stage 1 axons (**right**, n=9 mice, 155 axons) in EAE lesions before ('pre') and after ('4h- BEP') pharmacological inhibition of the NCX (bepridil 0.1 mM) over 4 hours. **Top:** Percentage of axons with $[Ca^{2+}]_{cyt} \geq 3$ SD above control mean, shown as mean ± SEM. Analyzed by paired t-test, tested per animal. (**B**) $[Ca^{2+}]_{cyt}$ of single axons plotted as YFP/CFP ratios. Stage 0 (**left**, n=4 mice, 564 axons) and stage 1 (**right**, n=4 mice, 203 axons) axons in EAE lesions before ('pre') and after ('4h-LOM') pharmacological inhibition of L-type and T-type calcium channels (lomerizine 0.1 mM) over 4 hours. **Top:** Percentage of axons with $[Ca^{2+}]_{cyt} \geq 3$ SD above control mean, shown as mean ± SEM. Analyzed by paired t-test, tested per animal. (**C**) **Left:** Distribution of axonal stages after application of a nitric oxide donor ('NO', spermine NONOate 50 mM, 60 min, n=3 mice, 90 axons) and after co-application of a nitric oxide donor and a NCX-inhibitor ('NO+BEP', spermine NONOate 50 mM, bepridil 0.1 mM, 60 min, n=3 mice, 90 axons) on a healthy spinal cord. **Right:** Fate of $[Ca^{2+}]_{cyt}$-high stage 0 (n=8 vs. 9 mice, 146 axons) and stage 1 (n=8 vs. 9 mice, 184 axons) axons in EAE lesions before ('Pre') and after ('4h') bath-application of vehicle or bepridil. While the NCX-inhibitor bepridil effectively blocks calcium influx (see panel **A**) and axon degeneration induced by NO, it does not prevent axonal damage in EAE lesions. Analyzed by chi-square test. (**D**) Fate of $[Ca^{2+}]_{cyt}$-high stage 0 (n=4 vs. 3 mice, 150 axons) and stage 1 (n=4 vs. 3 mice, 137 axons) axons before ('Pre') and after ('4h') bath-application of vehicle or lomerizine. No marked or consistent protective effect of lomerizine treatment was observed. Analyzed by chi-square test. (**E**) *In vivo* multiphoton projection image of a healthy spinal cord as ratiometric (YFP/CFP) images color-coded for axonal $[Ca^{2+}]_{cyt}$, shown before (**top:** 'pre glutamic acid') and after (**bottom:** 'post glutamic acid') application of glutamic acid (100 mM, glycine 10 mM) over 4 hours. Asterisk indicates neuronal soma. (**F**) Percentage of axons or neuronal somata with $[Ca^{2+}]_{cyt} \geq 3$ SD above control mean, shown as mean ± SEM (**top**, tested per animal in n=3 mice, respectively, paired t-test). **Bottom:** $[Ca^{2+}]_{cyt}$ of single axons or somata plotted as YFP/CFP ratios before ('Pre') and after bath-application of glutamic acid (**left**, '4h-Glu', glutamic acid 100 mM, glycine 10 mM, 4 hours) or glutamate receptor agonists (**right,** '2h-GluAg', NMDA 1 mM, glycine 0.1 mM, kainate 2 mM, AMPA 1mM, 2 hours) (**G**) Distribution of axonal stages before ('Pre') and after application of glutamic acid (**left**, '4h-Glu', 4 hours, n=3 mice, 90 axons) or glutamate agonists (**right,** '2h-GluAg', NMDA 1 mM, glycine 0.1 mM, kainate 2 mM, AMPA 1mM, 2 hours, n=3 mice, 90 axons). *P < 0.05; ***P < 0.001. Scale bar in **E,** 25 μm.

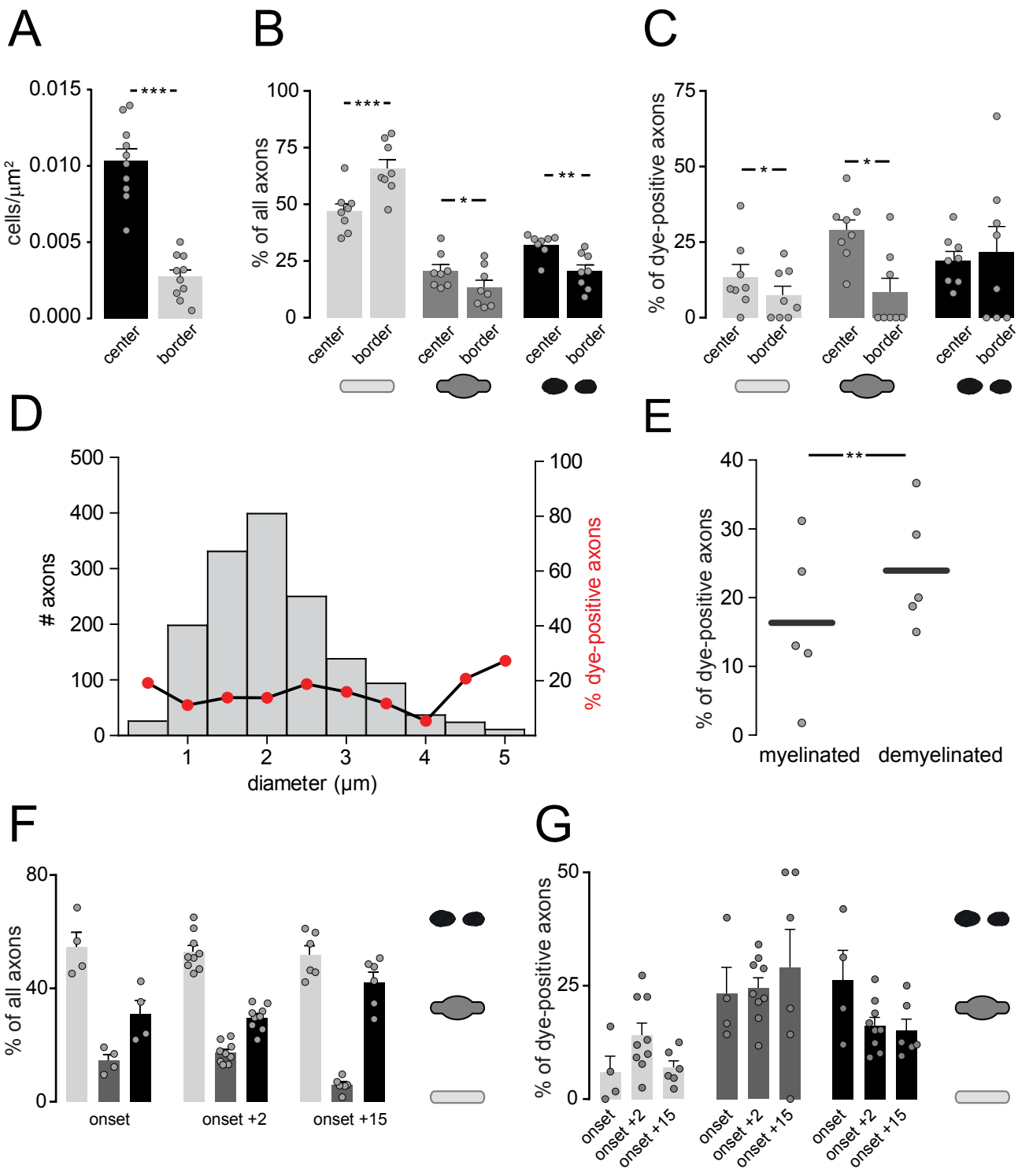

Figure S5 – Influence of inflammation and demyelination on nanorupture formation *(related to Fig. 4)*

(A) Quantification of cell density in the lesion core ('center') and outer rim ('border') of the same spinal EAE lesions (n=10 mice, mean + SEM, paired t-test). (**B**) Distribution of axonal stages (from **left** to **right**: stage 0, stage 1, stage 2) in spinal cord lesion 'center' and 'border' of EAE animals (n=8 mice, mean + SEM, analyzed by paired t-test for stages 0, 1 and Wilcoxon signed rank test for stage 2 axons). (**C**) Percentage of Texas Red-labeled dextran 3 kD dye-positive axons in EAE lesion 'center' and 'border' (n=8 mice, mean + SEM, analyzed by paired t-test for stages 0 and 2 and Wilcoxon signed rank test for stage 1). (**D**) Histogram relating the size of morphologically unaffected axons to their probability to

take up dye (in %, red dots) in acute EAE lesions (n=9 mice, 1519 axons). (**E**) Quantitative analysis of the percentage of myelinated and demyelinated intact axons (axon stages 0 and 1) that show uptake of dye in acute EAE lesions (n=5 mice, paired t-test). (**F**) Distribution of axonal stages in EAE in animals at onset, 2d and 15d after onset (n=4, 9 and 6 mice, respectively, mean + SEM). (**G**) Percentage of dye-positive axons in animals at onset, 2d and 15d after onset (n=4, 9 and 6 mice, respectively, mean + SEM; onset+2 data re-plotted from **Fig. 4B**). *P < 0.05; **P < 0.01; ***P < 0.001.